Integral Geometry and Geometric Probability in Plane

Hiroshi Saito

1 Introduction

Integral geometry is the theory that applies probabilistic ideas to geometric problems. On the other hand, information and communication technologies have recently started to be investigated regarding spatial and geometrical events or phenomena in the plane. Coverage of wireless and sensor systems is a typical example. Thus, integral geometry and derived geometric probability is a good tool to investigate such topics. However, it is not well known. In this report, I briefly explain integral geometry and geometric probability in the plane. Integral geometry is valid in a general Euclidean space. Even for a non-Euclidean space, it is extended [16]. However, this report focuses on the Euclidean plane. This is because (1) many practical problems can be treated as problems in the Euclidean plane, (2) the results obtained by integral geometry for the plane are simple and useful, and (3) integral geometry for the plane does not require mathematically advanced knowledge.

Integral geometry is sometimes confused with stochastic geometry [1], [17], which has been used in many papers regarding the performance analysis of wireless systems. Stochastic geometry models mobile terminals as a stochastic point process on the plane and analyzes the interference between these terminals. To derive an explicit result, stochastic geometry normally involves an isotropic path-loss function. This means that a region in which a received signal power is larger than a threshold becomes a disk. However, integral geometry involves a geometric object as a model and is appropriate for performance analysis on the impact of the object's shape.

2 Applications of integral geometry

Research on sensor networks or wireless networks has been done using integral geometry and geometric probability. References [4] and [5] directly applied the results of integral geometry discussed in Chapter 5 and Section 6.7 in [16] to the analysis of detecting an object moving in a straight line and to the evaluation of the probability of k-coverage. In addition, reference [3] applied integral geometry to the analysis of straight line routing, which is an approximation of shortest path routing, and reference [2] uses it to operate sensors in an energy-conserving way. Reference [15] investigated target detection, barrier coverage, and path coverage with randomly deployed sensors and analyzed the relationship between the performance and sensing area shape. The surface coverage of a 3D space was investigated [18], and WiFi coverage to offload the cellular traffic was analyzed [13]. Reference [30] used the formulas regarding the n-dimensional volume of a cell and the $(n-1)$-dimensional unit sphere surface to compute the mean received power. Furthermore, target shape estimation using binary sensory data was investigated by using integral geometry and geometric probability [7], [8], [9], [10].

Another important research field is disaster management for networks. Neumayer et al. [6] derived the polynomial time algorithm to evaluate metrics for a line-segment network model and a line disaster model. Other studies [11], [14], [12] proposed a network design method that is robust against disasters and minimizes the probability that a network will intersect a disaster area or be disconnected, although they do not emphasize integral geometry.

Other important applications are in image processing and computer graphics and physics. Examples of the former are [19], [20], [21], [22], [23], [24] and those of the latter are [25], [26], [27], [28]. There has been little but important research in simulation studies, e.g., [29].

3 Notations

In the remainder of this paper, for a set $X \subset \mathbb{R}^2$, $|X|$ denotes the perimeter length of X, $\|X\|$ denotes the size of X, $\overline{X}$ denotes the convex hull of X, and ∂X denotes the boundary of X. In addition, for a given line G, $\sigma(X)$ denotes the length of the chord $X \cap G$. For regions $X, Y \subset \mathbb{R}^2$, $l_{\partial X \cap Y}$ denotes the length of the arc created by ∂X and Y, that is, the part of ∂X included in Y.

4 Geometric probability

I introduce the concepts of geometric probability [16] through integral geometry.

Consider a bounded set $X \subset \mathbb{R}^2$ and a condition X_c. The position of X is characterized by the position of its reference point (x, y) and by its angle θ formed by a reference line fixed to X with another reference line fixed to the fixed coordinates, [Fig. 1-(a)], where (x, y, θ) is within a fixed parameter domain Ω. We can define a

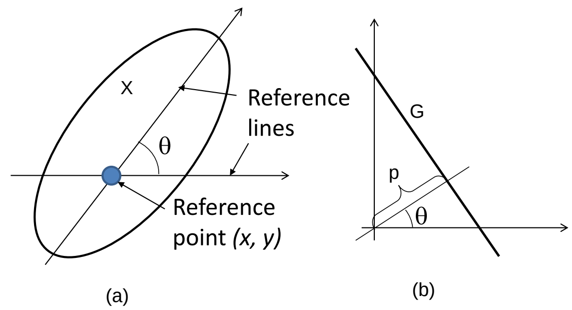

Fig. 1. Parameterization

probability that a set of positions of X satisfies a certain condition X_c. A typical example of X_c is $X \cap Y \neq \emptyset$ for a given Y. When (x, y) and θ are uniformly distributed, this probability is given by the ratio of the size of the subspace $\{(x, y, \theta)|(x, y, \theta)$ satisfies $X_c\}$ to the size of Ω. That is, the probability that a set of positions of X satisfies X_c is $\int_{X_c} dX / \int_\Omega dX$, where $dX = dx\, dy\, d\theta$. The definition of this probability is quite natural and intuitive because (x, y) and θ are uniformly distributed. Roughly speaking, when X moves and takes all the positions defined by $\{(x, y, \theta)|(x, y, \theta)$ satisfies $\Omega\}$, the ratio of the position of X satisfying X_c is this probability. This probability is formally called a "geometric probability," and its definition is based on integral geometry [16]. Here, $m(X : X_c) \stackrel{\text{def}}{=} \int_{X_c} dX$, called the measure of the set of positions of X satisfying condition X_c, is a non-normalized probability because it is proportional to the probability and normalized by $m(X : \Omega)$. (In integral geometry, the notation $dX = dx \wedge dy \wedge d\theta$ is often used. Here, $\wedge$ denotes the symbol of the exterior product and is convenient when we transform the coordinates. However, we can ignore this symbol and consider the equation below as a normal Lebesgue integral because we do not transform the coordinates here.)

The most important feature of the measure defined by integral geometry is that the measure must be invariant under the group of motions (translation and rotation) in the plane. As a result, convenient parameterization exists to describe a certain class of X. For a bounded X, we can use the natural parameterization (x, y, θ).

Similarly to the definition of probability, we can also define an expectation. For each position (x, y, θ) of X, we define a quantity $q(X) = q(x, y, \theta)$. Then, its expectation $E[q(X)]$ is defined by $\int_\Omega q(X) dX / \int_\Omega dX$.

When X is a line G, we use the parameterization by the angle θ the direction perpendicular to G makes with a fixed direction ($-\pi \leq \theta \leq \pi$) and by its distance p from the origin O ($0 \leq p$) [Fig. 1-(b)]. (We can use another parameterization, but we cannot calculate the integral uniformly over the possible parameter space X_c when the parameters θ and p are not used. This is because integral geometry requires the calculated results to be invariant under the group of motions in the plane.) By using θ and p, the expectation of the quantity $q(G)$ is calculated by $\int_\Omega q(G) dG / \int_\Omega dG = \int_\Omega q(G) dp\, d\theta / \int_\Omega dp\, d\theta$.

5 Known basic formulas

In many applications in the plane, it is often the case that combinations of the known explicit formulas below can solve problems of interest.

5.1 Formulas regarding bounded finite sets

This subsection provides formulas related to bounded finite sets that take various positions in the plane.

5.1.1

For a fixed convex set X_0, the measure of the set of positions of a convex set X_1 that meets X_0 is given as follows (Eq. (6.48) in [16]).

$$\int_{X_0 \cap X_1 \neq \emptyset} dX_1 = 2\pi(\|X\| + \|Y\|) + |X| \cdot |Y| \quad (1)$$

Particularly when X_0 is a point, Eq. (1) becomes

$$\int_{X_0 \cap X_1 \neq \emptyset} dX_1 = 2\pi \|X_1\|. \quad (2)$$

This formula is valid even when X_1 is not convex.

5.1.2

For a fixed convex set X_0, the measure of the set of positions of a convex set X_1 that is contained in X_0 is given as follows (Eq. (6.52) in [16]).

$$\int_{X_1 \subset X_0} dX_1 = 2\pi(\|X_0\| + \|X_1\|) - |X_0| \cdot |X_1| \quad (3)$$

Formally speaking, additional conditions on the curvature of ∂X_0 and that of ∂X_1 are needed for Eq. (3).

5.1.3

For a fixed set X_0, the integral of $\|X_0 \cap X_1\|$ over the position of the set of X_1 is given as follows (Eq. (4) is Eq. (6.57) in [16]. Although Eq. (6.57) in [16] does not include π, Eq. (4) is correct and original Eq. (6.57) in [16] is incorrect.).

$$\int_{X_0 \cap X_1 \neq \emptyset} \|X_0 \cap X_1\| dX_1 = 2\pi \|X_0\| \cdot \|X_1\| \quad (4)$$

5.1.4

Due to Eq. (6.61) in [16],

$$\int_{X_0 \cap X_1 \neq \emptyset} l_{\partial X_1 \cap X_0} dX = 2\pi |X_1| \|X_0\| \quad (5)$$

5.1.5

Assume that a curve r consists of n line segments. Let $\phi_i \leq \pi$ be the inner angle of the i-th and $(i+1)$-th line segments ($i = 1, 2 \cdots, n-1$). According to [12], for a convex set X,

$$\begin{aligned} \int_{r \cap X \neq \emptyset} dX &= |X| \cdot |r| + 2\pi \|X\| - \sum_i f(\phi_i) \\ &\leq |X| \cdot |r| + 2\pi \|X\|. \end{aligned} \quad (6)$$

When $|r|$ is fixed, $f(\phi_i)$ is a decreasing function of $\phi_i \leq \pi$. Formally, r needs to satisfy some mathematical conditions [12].

5.1.6

For a line segment l of length L and a convex set X, the approximation formula is proposed [12].

$$\int_{l\subset X} dX \approx \begin{cases} g_1(L, \frac{|X|}{2\pi}), & \text{if } |X|^2 < 16\|X\| \\ g_2(L, a, b), & \text{if } |X|^2 \geq 16\|X\|, \end{cases} \qquad (7)$$

$$\begin{aligned} a &= (|X| - \sqrt{|X|^2 - 16\|X\|})/4, \\ b &= (|X| + \sqrt{|X|^2 - 16\|X\|})/4, \end{aligned}$$

$$\begin{aligned} & g_1(L, R) \\ \stackrel{\text{def}}{=} & \begin{cases} 4\pi\{R^2 \arccos(\frac{L}{2R}) - \frac{LR}{2}\sqrt{1 - (\frac{L}{2R})^2}\}, & \text{for } L < 2R, \\ 0, & \text{otherwise} \end{cases} \end{aligned}$$

For $L \leq a$,

$$g_2(L, a, b) \stackrel{\text{def}}{=} 2\pi ab + 2L^2 - 4L(a + b),$$

for $a \leq L \leq b$,

$$\begin{aligned} & g_2(L, a, b) \\ \stackrel{\text{def}}{=} & 4ab(\pi/2 - \arccos(\frac{a}{L})) - 4Lb + 4b\sqrt{L^2 - a^2} - 2a^2, \end{aligned}$$

for $b \leq L \leq \sqrt{a^2 + b^2}$,

$$\begin{aligned} & g_2(L, a, b) \\ \stackrel{\text{def}}{=} & 4ab(\pi/2 - \arccos(\frac{b}{L}) - \arccos(\frac{a}{L})) \\ & +4a\sqrt{L^2 - b^2} + 4b\sqrt{L^2 - a^2} \\ & -2b^2 - 2a^2 - 2L^2, \end{aligned}$$

and for $\sqrt{a^2 + b^2} < L$, $g_2(L, a, b) \stackrel{\text{def}}{=} 0$.

5.1.7

There is a rectangle of which side lengths are L and w. Let G_1 and G_2 be the sides of lengths L. The directions of G_1 and G_2 are defined to be the same, and G_1 is located to the right and G_2 to the left when their tails are at the bottom. On each G_1 and G_2, n marks are placed at equal intervals l, where $L = l(n - 1)$ [Fig. 2-(a)]. These marks on both G_1 and G_2 are numbered in increasing order from the head to the tail of them. The first mark is located at the head and the n-th mark is located at the tail.

There is a vertex of which the interior angle is α. For $1 < i_1 \leq j_1 < n$, $1 < i_2 \leq j_2 < n$, and $\alpha < \pi$, define the measure $\tilde{m}(\alpha, i_1, j_1, i_2, j_2|l, n, w)$ of a set of positions of the rectangle satisfying the following: Marks $i_1, \cdots, j_1$ on G_1 and marks $i_2, \cdots, j_2$ on G_2 are inside the vertex and other marks are outside it [Fig. 2-(b)].

Then, $\tilde{m}(\alpha, i_1, j_1, i_2, j_2|l, n, w)$ is given as follows [8].

$$\begin{aligned} & \tilde{m}(\alpha, i_1, j_1, i_2, j_2|l, n, w) \\ = & \begin{cases} m(\alpha, i_1, j_1, i_2, j_2|l, n, w) & \text{for } j_1 - i_1 > j_2 - i_2, \\ m(\alpha, i_1, j_1, i_2, j_2|l, n, w) & \\ +m(\alpha, i_2, j_2, i_1, j_1, |l, n, w) & \text{for } j_1 - i_1 = j_2 - i_2 \\ m(\alpha, i_2, j_2, i_1, j_1|l, n, w) & \text{for } j_1 - i_1 < j_2 - i_2. \end{cases} \end{aligned} \qquad (8)$$

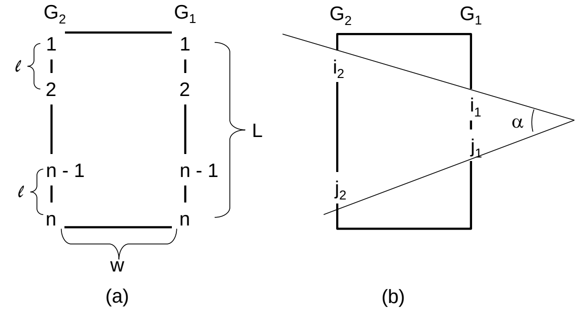

Fig. 2. Rectangle with marks

$$\begin{aligned} & m(\alpha, i_1, j_1, i_2, j_2|l, n, w) \\ = & \sum_{i,j=0,1} \frac{\mathbf{1}(u_{i,j} > l_{i,j})}{4\sin\alpha} \\ & \{\eta_{1,i,j}(\sin(2u_{i,j} - \alpha) - \sin(2l_{i,j} - \alpha)) \\ & +\eta_{2,i,j}(\cos(2u_{i,j} - \alpha) - \cos(2l_{i,j} - \alpha)) \\ & +\eta_{3,i,j}(u_{i,j} - l_{i,j})\} \end{aligned} \qquad (9)$$

Here,

$$\begin{aligned} c(k|i) &\stackrel{\text{def}}{=} (-1)^k i - 1 \\ \eta_{1,i,j} &\stackrel{\text{def}}{=} (-1)^{i+j+1}w^2 + c(i|j_0)c(j|i_0)l^2 \\ \eta_{2,i,j} &\stackrel{\text{def}}{=} (-1)^j c(i|j_0)lw + (-1)^i c(j|i_0)lw \\ \eta_{3,i,j} &\stackrel{\text{def}}{=} 2\{(-1)^{i+j}w^2 + c(i|j_0)c(j|i_0)l^2\}\cos\alpha \\ & \quad +2\{(-1)^j c(i|j_0) - (-1)^i c(j|i_0)\}lw\sin\alpha \\ i_0 &\stackrel{\text{def}}{=} i_1 - i_2 \\ j_0 &\stackrel{\text{def}}{=} j_1 - j_2 \\ l_{i,j} &\stackrel{\text{def}}{=} \max[\tan^{-1}((j_0 - \mathbf{1}(i = 0))l/w), \\ & \qquad \alpha + \tan^{-1}((i_0 - \mathbf{1}(j = 0))l/w)] \\ u_{i,j} &\stackrel{\text{def}}{=} \min[\tan^{-1}((j_0 + \mathbf{1}(i = 1))l/w), \\ & \qquad \alpha + \tan^{-1}((i_0 + \mathbf{1}(j = 1))l/w)]. \end{aligned}$$

For $\alpha > \pi$, we can also obtain a similar result.

5.2 Formulas regarding lines

This subsection provides formulas related to lines that take various positions in the plane.

5.2.1

According to Eqs. (3.12) and (3.6) in [16], for a fixed convex set C, the measure in which the set of positions of a line G that meets C is given by

$$\int_{C\cap G\neq\emptyset} dG = |C|, \qquad (10)$$

and the (non-normalized) mean length of the chord made by C and G is given by

$$\int_{C\cap G\neq\emptyset} \sigma(C)dG = \pi\|C\|. \qquad (11)$$

5.2.2

When $C_1 \cap C_2 = \emptyset$, we can define the internal cover $C_1 \otimes C_2$ of C_1 and C_2 by a closed elastic string drawn around C_1 and C_2 and crossing over at a point placed between them (Fig. 3). Due to the result on p.33 in [16], the following formula for convex sets C_1 and C_2 is given by [11].

$$\begin{aligned} & \int_{G\cap C_1=\emptyset, G\cap C_2=\emptyset, G\cap\overline{C_1\cup C_2}\neq\emptyset} dG \\ = \; & |C_1 \otimes C_2| - |C_1| - |C_2|. \end{aligned} \tag{12}$$

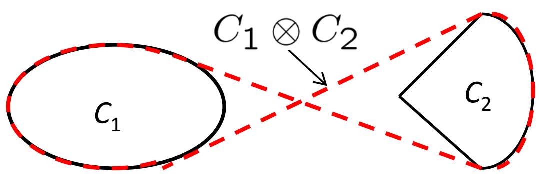

Fig. 3. Internal cover $C_1 \otimes C_2$ of C_1 and C_2

5.2.3

As a special case given by [14], the following formula is obtained. For a set $C \subseteq X$,

$$\int_{R_G\cap C\neq\emptyset, G\cap X\neq\emptyset} dG = |\overline{C}| + |X|, \tag{13}$$

where R_G is the right-half plane (the plane of the right side) of G and X is convex.

6 Property

Similar to the discussion in [13], we can obtain the following property.

Assume that a region A is divided into sub-regions $\{A_i\}_i$, where $A_i \cap A_j = \emptyset$ for any $j \neq i$, $\cup_i A_i = A$. Here, A_i is divided into convex micro-regions $\{A_{i,j}\}_j$, where $A_{i,j} \cap A_{i,k} = \emptyset$ for any $j \neq k$, $\cup_j A_{i,j} = A_i$. An environment value h_i, such as temperature, is defined at A_i. There is a randomly placed line G (a randomly placed finite length curve C) intersecting A. A point s is moving on G (C) at a unit speed. Let H be the expected environment value of a randomly placed point s in A. Let H_G (H_C) be the time-average environment value of a point s moving on G (C). Then, $H = H_G = H_C$.

Proof: It is clear

$$H = \sum_i h_i \Pr(s \subset A_i) = \sum h_i \|A_i\|/\|A\|. \tag{14}$$

In addition,

$$H_G = \int_{A\cap G\neq\emptyset} \sum_{i,j} h_i \sigma(A_{i,j}) dG \Big/ \int_{A\cap G\neq\emptyset} \sigma(A) dG. \tag{15}$$

Due to Eq. (11),

$$H_G = \sum_{i,j} h_i \|A_{i,j}\|/\|A\| = \sum_i h_i \|A_i\|/\|A\|. \tag{16}$$

On the other hand,

$$H_C = \frac{\int_{A\cap C\neq\emptyset} \sum_{i,j} h_i \int_{s\subset(A_{i,j}\cap C)} ds\, dC}{\int_{A\cap C\neq\emptyset} \sum_{i,j} \int_{s\subset(A_{i,j}\cap C)} ds\, dC}. \tag{17}$$

Based on the discussion in Appendix in [13],

$$\int_{A_{i,j}\cap C\neq\emptyset, s\subset(A_{i,j}\cap C)} ds\, dC = \pi|C| \cdot \|A_{i,j}\|. \tag{18}$$

Because $A_{i,j} \cap C = \emptyset$, $\int_{s\subset(A_{i,j}\cap C)} ds\, dC = 0$. Therefore, $\int_{A\cap C\neq\emptyset, s\subset(A_{i,j}\cap C)} ds\, dC = \int_{A_{i,j}\cap C\neq\emptyset, s\subset(A_{i,j}\cap C)} ds\, dC$. Hence,

$$\int_{A\cap C\neq\emptyset, s\subset(A_{i,j}\cap C)} ds\, dC = \pi|C| \cdot \|A_{i,j}\|. \tag{19}$$

As a result,

$$H_C = \frac{\sum_{i,j} h_i \|A_{i,j}\|}{\sum_{i,j} \|A_{i,j}\|} = \sum_i h_i \|A_i\|/\|A\|. \tag{20}$$

References

[1] F. Baccelli and B. Blaszczyszyn, Stochastic geometry and wireless networks, NOW, Boston, 2009.

[2] W. Choi and S. K. Das, A Novel Framework for Energy-Conserving Data Gathering in Wireless Sensor Networks, INFOCOM2005, pp. 1985–1996, 2005.

[3] S. Kwon and N. B. Shroff, Analysis of Shortest Path Routing for Large Multi-hop Wireless Networks, IEEE/ACM Trans. Networking, 17, 3, pp. 857–869, 2009.

[4] L. Lazos and R. Poovendran, Stochastic Coverage in Heterogeneous Sensor Networks, ACM Transactions on Sensor Networks, 2, 3, pp. 325–358, 2006.

[5] L. Lazos, R. Poovendran, and J. A. Ritcey, Probabilistic Detection of Mobile Targets in Heterogeneous Sensor Networks, IPSN07, pp. 519–528, 2007.

[6] S. Neumayer and E. Modiano, Network reliability with geographically correlated failures, in Proc. IEEE INFOCOM, 2010.

[7] H. Saito, K. Shimogawa, S. Shioda, and J. Harada, Shape Estimation Using Networked Binary Sensors, INFOCOM, pp. 2901 - 2905, 2009.

[8] H. Saito, S. Tanaka, and S. Shioda, Stochastic Geometric Filter and Its Application to Shape Estimation for Target Objects, IEEE Trans. Signal Processing, 59, 10, , pp. 4971-4984, 2011.

[9] H. Saito, S. Shimogawa, S. Tanaka, and S. Shioda, Estimating Parameters of Multiple Heterogeneous Target Objects Using Composite Sensor Nodes, IEEE Trans. Mobile Computing, 11, 1, pp. 125-138, 2012.

[10] H. Saito and S. Shioda, Parameter Estimation Method for Time-variant Target Object Using Randomly Deployed Sensors and its Application to Participatory Sensing, IEEE Trans. Mobile Computing, 14, 6, pp. 1259-1271, 2015.

[11] H. Saito, Geometric Evaluation of Survivability of Disaster-affected Network with Probabilistic Failure, INFOCOM, pp. 1608 - 1616, 2014.

[12] H. Saito, Spatial Design of Physical Network Robust against Earthquakes, IEEE Journal of Lightwave Technology, 33, 2, pp.443-458, 2015.

[13] H. Saito et al., Geometrical Characterization of Offloading through Wireless LANs, IEEE Trans. Mobile Computing, to appear.

[14] H. Saito, Analysis of Geometric Disaster Evaluation Model for Physical Networks, IEEE Trans. Networking, 23, 6, pp. 1777-1789, 2015.

[15] H. Saito, Theoretical Optimization of Sensing Area Shape for Target Detection, Barrier Coverage, and Path Coverage, IEICE Trans. Commun., to appear.

[16] L. A. Santaló, Integral Geometry and Geometric Probability, Second edition. Cambridge University Press, Cambridge, 2004.

[17] S. Weber, J. G. Andrews, and N. Jindal, An Overview of the Transmission Capacity of Wireless Networks, IEEE Trans. Commun., 58, 12, pp.3593-3604 , 2010.

[18] M. Zhao, J. Lei, M. Wu, Y. Liu, and W. Shu, Surface Coverage in Wireless Sensor Networks, INFOCOM, 2009.

[19] K. Michielsen and H. De. Raedt, Integral-geometry morphological image analysis, Physics Reports, 347, 6, 2001, pp. 461-538, 2001.

[20] Y. Boykov and V. Kolmogorov, Computing geodesics and minimal surfaces via graph cuts, Computer Vision, 2003.

[21] Frederic Cazals and Mateu Sbert, Details, Some Integral Geometry Tools to Estimate the Complexity of 3D Scenes, hal.inria.fr (Open Archive of INRIA), 1997.

[22] J. Levy Vehel, About lacunarity, some links between fractal and integral geometry, and an application to texture segmentation, Computer Vision, 1990.

[23] D. J. H. Moore, An Approach to the Analysis and Extraction of Pattern Features Using Integral Geometry, IEEE Transactions on Systems, Man, and Cybernetics, 2 , 1, pp. 97-102, 1972.

[24] G. Tenery, A pattern recognition function of integral geometry, IEEE Transactions on Military Electronics, 7, 2-3, pp. 196-199, 1963.

[25] Klaus R. Mecke, Integral Geometry in Statistical Physics, International Journal of Modern Physics B, 12, 9, 1998.

[26] J. Raczkowska, J. Rysz, A. Budkowski, J. Lekki, M. Lekka, A. Bernasik, K. Kowalski, and P. Czuba, Macromolecules, 36, 7, pp. 2419-2427, 2003. Nuclear physicas:

[27] A. Mazzolo, B. Roesslinger, and C. M. Diop, On the properties of the chord length distribution, from integral geometry to reactor physics, Annals of Nuclear Energy, 30, 14, pp. 1391-1400, 2003. Geophysics:

[28] T. F. Stepinski and S. Coradetti, Comparing morphologies of drainage basins on Mars and Earth using integral-geometry and neural maps, Geophysical research letters, DOI: 10.1029/2004GL020359, 2004.

[29] Mateu Sbert, An Integral Geometry Based Method for Fast Form-Factor Computation, Computer Graphics Forum, 12, 3, pp. 409-420, 1993.

[30] J. Hansen and M. Reitzner, Efficient indoor radio channel modeling based on integral geometry, IEEE Transactions on Antennas and Propagation, 52, 9, pp. 2456-2463, 2004.